THE JOURNAL OF BIOLOGICAL CHEMISTRY
Vol. 279, No. 28, Issue of July 9, pp. 29450–29460, 2004
Printed in U.S.A.

Positive Regulation of Phagocytosis by SIRPβ and Its Signaling Mechanism in Macrophages*

Received for publication, January 28, 2004, and in revised form, April 27, 2004
Published, JBC Papers in Press, May 3, 2004, DOI 10.1074/jbc.M400950200

Akiko Hayashi‡§, Hiroshi Ohnishi‡, Hideki Okazawa‡, Seshiru Nakazawa‡, Hiroshi Ikeda‡, Sei-ichiro Motegi‡, Naoko Aoki¶, Shoji Kimura‖, Masahiko Mikuni§, and Takashi Matozaki‡

From the ‡Biosignal Research Center, Institute for Molecular and Cellular Regulation, Gunma University, 3-39-15 Showa-Machi, Maebashi, Gunma 371-8512, the §Department of Psychiatry and Human Behavior, Gunma University Graduate School of Medicine, 3-39-22 Showa-Machi, Maebashi, Gunma 371-8511, and the ¶Department of Pathology and ‖School of Nursing, Asahikawa Medical College, Higashi 2-1-1, Midorigaoka, Asahikawa 078-8510, Japan

SIRPβ (signal-regulatory protein β) is a transmembrane protein that is expressed in hematopoietic cells but whose functions are unknown. We have now cloned mouse SIRPβ cDNA and have shown that the gene is expressed in various tissues in addition to cells of the macrophage lineage. Engagement of SIRPβ by specific monoclonal antibodies promoted Fcγ receptor-dependent or -independent phagocytosis in mouse peritoneal macrophages. It also induced marked activation of MAPK and the upstream kinase MEK but weak activation of Akt. MEK inhibitors markedly blocked the promotion of phagocytosis by SIRPβ, whereas an inhibitor of phosphoinositide 3-kinase partly blocked such response. In addition, inhibitors of myosin light chain kinase or of myosin ATPase blocked the promotion of phagocytosis by SIRPβ. Furthermore, SIRPβ induced the formation of filopodia and lamellipodia in macrophages as well as the translocation of activated MAPK to these structures. It also elicited tyrosine phosphorylation of DAP12, Syk, and SLP-76, and a Syk inhibitor blocked the promotion of phagocytosis and activation of MAPK by SIRPβ. Our results suggest that engagement of SIRPβ promotes phagocytosis in macrophages by inducing the tyrosine phosphorylation of DAP12, Syk, and SLP-76 and the subsequent activation of a MEK-MAPK-myosin light chain kinase cascade.

Macrophages recognize, phagocytose, and thereby eliminate microbial pathogens, apoptotic or necrotic cell corpses, and chemically modified lipoproteins (1–3). Various receptors responsible for the specific recognition of targets for phagocytosis by macrophages have been identified (2, 4). The best characterized of these receptors is the Fcγ receptor (FcγR),[1] which recognizes the Fc region of IgG bound to antigen presented on microbial pathogens (5, 6). The cross-linking of FcγRs by the Fc region of IgG induces tyrosine phosphorylation by an Src family kinase of the receptors themselves and of associated proteins that contain an immunoreceptor tyrosine-based activation motif (ITAM) (5, 6). The phosphorylated ITAM then serves as a docking site for the tyrosine kinase Syk. Downstream signaling mediated by phosphoinositide (PI) 3-kinase or Rho family small GTP-binding proteins eventually triggers phagocytosis of IgG-coated (opsonized) particles (5, 7–10).

SIRPβ (signal-regulatory protein β) is a transmembrane protein that possesses three Ig-like domains in its extracellular region and a short cytoplasmic tail (11). It was initially discovered on the basis of its homology to another transmembrane protein, named SHP substrate-1 (SHPS-1) or SIRPα (11). Human SIRPβ is expressed in monocytes and granulocytes but not in lymphocytes (12). SIRPβ forms a complex with DAP12 in human monocytes or transfected nonhematopoietic cells (13, 14). DAP12 is a transmembrane protein that was originally identified on the basis of its association with the inhibitory receptors of natural killer cells (15, 16). Its intracellular region contains a single ITAM motif, which binds Syk or the tyrosine kinase ZAP-70. The association between SIRPβ and DAP12 is thought to be mediated by an ionic interaction between single amino acids of opposite charge (lysine of SIRPβ and aspartic acid of DAP12) within the transmembrane regions (13, 14, 17). Ligation of SIRPβ resulted in the tyrosine phosphorylation of DAP12 and the subsequent recruitment of Syk to the SIRPβ-DAP12 complex in RBL-2H3 cell transfectants (14). It also stimulated serotonin release from these cells (14). SIRPβ is therefore implicated as a positive regulator of hematopoietic cells.

In contrast to SIRPβ, the function of the related SHPS-1 (also known as SIRPα, P84, and BIT) is relatively well characterized (11, 18–20). SHPS-1 was initially discovered as a tyrosine-phosphorylated transmembrane protein that binds the SH2 domain-containing protein-tyrosine phosphatases SHP-1

* This work was supported by a grant-in-aid for scientific research on priority areas cancer, a grant-in-aid for scientific research (B), a 21st Century COE program grant from the Ministry of Education, Culture, Sports, Science, and Technology of Japan, a grant from the Uehara Memorial Foundation, a grant from the Brain Science Foundation, a grant from the Nakajima Foundation, and a grant from the Japan Research Foundation for Clinical Pharmacology. The costs of publication of this article were defrayed in part by the payment of page charges. This article must therefore be hereby marked "*advertisement*" in accordance with 18 U.S.C. Section 1734 solely to indicate this fact.

The nucleotide sequence(s) reported in this paper has been submitted to the DDBJ/GenBank™/EBI Data Bank with accession number(s) AB112022, AB112023, AB112024, and AB112025.

** To whom correspondence should be addressed: Biosignal Research Center, Institute for Molecular and Cellular Regulation, Gunma University, 3-39-15 Showa-Machi, Maebashi, Gunma 371-8512, Japan. Tel.: 81-27-220-8865; Fax: 81-27-220-8897; E-mail: matozaki@showa.gunma-u.ac.jp.

[1] The abbreviations used are: FcγR, Fcγ receptor; BDM, 2,3-butanedione 2-monoxime; Ig-sRBCs, IgG-opsonized sheep RBCs; ITAM, immunoreceptor tyrosine-based activation motif; mAb, monoclonal antibody; M-CSF, macrophage colony-stimulating factor; MLC, myosin light chain; MLCK, myosin light chain kinase; pAbs, polyclonal antibodies; PEM, peritoneal macrophage; PI, phosphoinositide; RACE, rapid amplification of cDNA ends; SHPS-1, SHP substrate-1; SPC, sphingosylphosphorylcholine; MAPK, mitogen-activated protein kinase; MEK, MAPK/extracellular signal-regulated kinase; GFP, green fluorescent protein; PBS, phosphate-buffered saline; FBS, fetal bovine serum; CHO, Chinese hamster ovary; RT, reverse transcriptase; RBC, red blood cells.

and SHP-2 and serves as their substrate (18, 21). The putative extracellular region of SHPS-1 contains three Ig-like domains, similar to SIRPβ, whereas the cytoplasmic region of this protein contains four Y*XX*(L/V/I) motifs, which are putative tyrosine phosphorylation sites and binding sites for the SH2 domains of SHP-1 and SHP-2 (11, 17, 18, 22). SHPS-1 is particularly abundant in macrophages and neurons (20, 23, 24), although it is also expressed in other cell types such as fibroblasts. CD47, a member of the Ig superfamily (25), is a ligand for SHPS-1 (24, 26), and CD47 and SHPS-1 appear to constitute a cell-cell communication system (the CD47-SHPS-1 system) in hematopoietic cells and other cell types. Indeed, the binding of CD47 on RBCs to SHPS-1 on macrophages inhibits phagocytosis of RBCs by macrophages (27, 28), suggesting that the CD47-SHPS-1 system contributes to self *versus* nonself recognition by macrophages. The binding of CD47 on T cells to SHPS-1 on dendritic cells also suppresses cytokine production by the dendritic cells (12).

We have now investigated the role of SIRPβ in macrophage function. We thus examined the effects of engagement of SIRPβ by specific monoclonal antibodies (mAbs) on phagocytosis as well as on intracellular signaling in macrophages.

EXPERIMENTAL PROCEDURES

Antibodies and Reagents—Rat mAbs and rabbit polyclonal antibodies (pAbs) to mouse SIRPβ were generated with a recombinant SIRPβ-Fc fusion protein (the extracellular region of mouse SIRPβ fused to the Fc region of human IgG) as antigen (see below). For the generation of mAbs, the purified SIRPβ-Fc protein was injected into the hind foot pads of two Wistar rats three times at 1-week intervals, after which lymphocytes were isolated from the draining lymph nodes and fused with P3U1 myeloma cells as described previously (21). Hybridoma clones producing mAbs that reacted with SIRPβ-Fc but not with SHPS-1-Fc were identified by enzyme-linked immunosorbent assay. Among several positive clones, clones 80 and 84 were selected for experiments. The mAbs were purified from serum-free culture supernatants of hybridoma cells by column chromatography on protein G-Sepharose 4FF (Amersham Biosciences). The isotype of both mAbs 80 and 84 was determined as IgG2a,κ with the use of a Rat MonoAB ID/SP kit (Zymed Laboratories Inc.). Rabbit pAbs to SIRPβ were purified from serum by column chromatography with SIRPβ-Fc conjugated to Sepharose and were then passed through a column of human IgG (Jackson ImmunoResearch) conjugated to Sepharose in order to remove antibodies that reacted with the human Fc portion of the antigen. Rabbit pAbs to DAP12 were generated as described previously (29). A mouse mAb to the Myc epitope tag (9E10) was purified from the culture supernatant of hybridoma cells. Rabbit pAbs to BLNK (for immunoprecipitation) were kindly provided by H. Yakura (Tokyo Metropolitan Institute for Neuroscience, Tokyo, Japan). Rabbit pAbs to MAPK and to active MAPK were from Promega; rabbit pAbs to MEK, to active MEK, to Akt, and to active Akt, and a mouse mAb to phosphotyrosine (PY-100) were from Cell Signaling Technology; rabbit pAbs to the phosphorylated form of myosin light chain (MLC), rabbit pAbs to Syk (N-19), rabbit pAbs to SLP-76 (H-300), and rabbit pAbs to BLNK (C-19, for immunoblot analysis) were from Santa Cruz Biotechnology. Isotype-matched control rat IgG (IgG2a,κ) was from Pharmingen. Rabbit pAbs to mouse RBCs were from Cedarlane Laboratories. A rat mAb (IgM) to mouse CD24 (J11d) was prepared from the culture supernatant of hybridoma cells. PD98059, ML-7, and sphingosylphosphorylcholine (SPC) were from Calbiochem; U0126 was from Promega; and wortmannin, 2,3-butanedione 2-monoxime (BDM), piceatannol, and a mouse mAb to MLC were from Sigma. Recombinant mouse macrophage colony-stimulating factor (M-CSF) was from R&D Systems.

Cloning of Mouse SIRPβ cDNAs—A full-length cDNA for C57BL/6 mouse SIRPβ was amplified by PCR from a λZapII spleen cDNA library (Stratagene) with the primers 5′-CCGGATCCAACAGGGTTCTTAACACCAACC-3′ (sense) and 5′-CCGAATTCTGCTCATTAGCACTTATTTCCA-3′ (antisense). The resulting PCR product was subcloned into pBluescript (Stratagene). A Balb/c mouse SIRPβ cDNA was amplified from a Marathon-Ready spleen cDNA library (Clontech) by 5′- and 3′-rapid amplification of cDNA ends (RACE)-PCR, with the primers 5′-CTCCTCAAGGGCAGATATGTTCACCAAGAGACA-3′ (antisense) and 5′-GTCTCCTATAGAGTTTCCAGCACAGT-3′ (sense) for the 5′- and 3′-RACE reactions, respectively. The resulting PCR product was subcloned into pGEM-T (Invitrogen). The nucleotide sequences of the amplified cDNAs were verified by sequencing with an ABI PRISM310 Genetic Analyzer (Applied Biosystems).

RT-PCR Analysis—Balb/c mouse SIRPβ cDNA fragments were amplified with the sense primer 5′- TGTGAAGTTCCAGAGAGGATCATCAGAGCC-3′ and the antisense primer 5′-TAGGTTCCAACACCACCTGGACTGTGCTGG-3′ and with first strand cDNAs generated from Balb/c mouse tissues (Clontech) as templates. First strand cDNAs were also prepared with a Superscript-based kit (Invitrogen) from total RNA that had been isolated from peritoneal macrophages (PEMs) and RAW264.7 cells. Glyceraldehyde-3-phosphate dehydrogenase cDNA fragments were simultaneously amplified from the same first strand cDNA preparations as an internal control.

Cells, Cell Culture, and Transfection—All cells were maintained at 37 °C under a humidified atmosphere of 5% CO_2 in air. CHO cells stably expressing an active form of H-Ras (CHO-Ras cells) were kindly provided by S. Shirahata (Kyushu University, Fukuoka, Japan). CHO-Ras cells expressing mouse SHPS-1 (30) were kindly provided by N. Honma (Kirin Brewery Co. Ltd., Gunma, Japan). CHO-Ras cells stably expressing mouse SIRPβ were generated as described below. These three cell lines were cultured in α-minimum Eagle's medium (Sigma) supplemented with 2 mM L-glutamine, 10 mM Hepes-NaOH (pH 7.4), 10% FBS, and geneticin (500 μg/ml) (Invitrogen). For CHO-Ras cells stably expressing mouse SIRPβ, the culture medium was also supplemented with Zeocin (250 μg/ml) (InvivoGen). The mouse macrophage cell line RAW264.7 (kindly provided by Y. Kaneko, Gunma University, Gunma, Japan) was cultured in RPMI 1640 (Sigma) supplemented with 10% FBS. GbaSM-4 cells, vascular smooth muscle cells derived from brain basilar arteries of guinea pigs (kindly provided by K. Kohama, Gunma University, Gunma, Japan), were cultured in Dulbecco's modified Eagle's medium (Sigma) supplemented with 10% FBS. Thioglycolate-elicited mouse primary PEMs were isolated and cultured as described (31). In brief, the peritoneum was flushed with ice-cold PBS 3 days after intraperitoneal injection of C57BL/6 mice with 2 ml of 3% thioglycolate broth (Nissui, Tokyo, Japan). The exudate cells were isolated by centrifugation at 400 × *g* for 5 min at 4 °C, washed with ice-cold RPMI 1640, and resuspended in RPMI 1640 supplemented with 10% FBS. After incubation for 24 h at 37 °C, nonadherent cells, which include neutrophils, B cells, and T cells, were washed away.

To examine the effect of a dominant-negative mutant of Syk on phagocytosis, RAW264.7 cells were cotransfected with a vector for GFP and a vector for kinase-negative porcine Syk (kindly provided by H. Yamamura, Kobe University, Hyogo, Japan) or the corresponding empty vector with the use of LipofectAMINE2000 (Invitrogen). Twenty four h after transfection, cells were subjected to phagocytosis assay as described below.

Generation of CHO-Ras Cells Expressing SIRPβ—A full-length C57BL/6 mouse SIRPβ cDNA was subcloned into the EcoRI site of pcDNA3.1 (Invitrogen). The resulting plasmid was then digested with EcoRV and NotI, rendered blunt-ended, and self-ligated to disrupt the EcoRV recognition sequence in the multiple cloning site. It was then subjected to PCR with the sense primer 5′-CCGATATCCGAGGAGGACCTGAGAGAGCTGAAAGTGATC-3′ and the antisense primer 5′-CCGATATCAGCTTCTGCTCTCTCACAGCTGCTCC-3′ to generate an expression plasmid for Myc epitope-tagged SIRPβ (with the Myc tag sequence inserted at the COOH terminus of the putative signal sequence of SIRPβ, between Arg^{29} and Glu^{30}). The PCR product was digested with EcoRV and self-ligated, and its nucleotide sequence was verified by DNA sequencing. The DNA fragment encoding Myc-SIRPβ was excised with ApaI and KpnI and then subcloned into pCAGGS (kindly provided by J. Miyazaki, Osaka University, Osaka, Japan). CHO-Ras cells were then transfected with pCAGGS-Myc-SIRPβ and pTracer-CMV (Invitrogen) containing a Zeocin resistance gene with the use of LipofectAMINE 2000 (Invitrogen). The transfected cells were cultured in α-minimum Eagle's medium supplemented with 2 mM L-glutamine, 10 mM Hepes-NaOH (pH 7.6), 10% FBS, geneticin (500 μg/ml), and Zeocin (500 μg/ml). Colonies were isolated 14–21 days after transfection. Several cell lines expressing Myc-SIRPβ were identified by immunoblot analysis of cell lysates with the 9E10 mAb to the Myc tag.

Preparation of SIRPβ-Fc and SHPS-1-Fc Fusion Proteins—For preparation of SIRPβ-Fc, a DNA fragment encoding the Fc portion was excised from the pEFneoFc76 vector (32) with EcoRI and NotI and was subcloned into pTracer-CMV to generate the vector pTracer-Fc. A DNA fragment encoding the extracellular region of SIRPβ (amino acids 1–362) was amplified from a full-length C57BL/6 mouse SIRPβ cDNA by PCR with the sense primer 5′-CCGGATCCAACAGGGTTCTTAACACCAACC-3′ and the antisense primer 5′-AGGTCTAGAAGCAATAC-

CTGCCGTCTTCA-3′. The PCR product was digested with BamHI and XbaI, and the resulting DNA fragment was subcloned into pTracer-Fc to generate the SIRPβ-Fc expression plasmid pTracer-CMV-SIRPβ-Fc. CHO-Ras cells were transfected with pTracer-CMV-SIRPβ-Fc and subjected to selection with Zeocin as described previously (32). Several cell lines producing SIRPβ-Fc were identified by immunoblot analysis of culture supernatants with horseradish peroxidase-conjugated goat pAbs specific for the Fc fragment of human IgG (Jackson Immuno Research). CHO-Ras cells producing a similar fusion protein of mouse SHPS-1 and the Fc portion of human IgG were also generated. The Fc fusion proteins produced by cells cultured in serum-free Dulbecco's modified Eagle's medium/F-12 (1:1) medium were purified from the culture supernatants by column chromatography on protein A-Sepharose 4FF (Amersham Biosciences).

Immunoprecipitation and Immunoblot Analysis—Cells were lysed for 1 h at 4 °C in a solution containing 50 mM Tris-HCl (pH 7.5), 150 mM NaCl, 1% Nonidet P-40, 10 mM NaF, 1 mM Na_3VO_4, 1 mM EDTA, 1 mM phenylmethylsulfonyl fluoride, and aprotinin (10 μg/ml). The lysates were centrifuged at 21,000 × *g* for 15 min at 4 °C, and the resulting supernatants were subjected to immunoprecipitation and immunoblot analysis. For immunoprecipitation, the supernatants were incubated for 4 h at 4 °C with antibodies bound to protein G-Sepharose beads. The beads were then washed twice with cell lysis buffer, resuspended in SDS sample buffer, and subjected to SDS-PAGE and immunoblot analysis. For detection of phosphorylated MLC, cells were treated with ice-cold trichloroacetic acid to precipitate all proteins. The pellets were then washed with ice-cold acetone containing 10 mM dithiothreitol, dried, and dissolved with urea sample buffer containing 20 mM Tris, 22 mM glycine, 10 mM dithiothreitol, and 8 M urea. Samples were then diluted with SDS sample buffer and subjected to SDS-PAGE and immunoblot analysis. Immune complexes were detected with an ECL detection kit (Amersham Biosciences).

Opsonization of Mouse RBCs—IgG- or C3bi-opsonized RBCs were prepared as described previously with minor modifications (28).

Cross-linking of SIRPβ for Phagocytosis Assay and Determination of Downstream Signaling—Thioglycolate-elicited mouse PEMs were plated in 24-well culture plates and cultured for 3–4 days. Immediately before phagocytosis assays, the plates were placed on ice and mAbs 80 or 84 to mouse SIRPβ (or isotype-matched control rat IgG) were then added to the cells at a concentration of 20 μg/ml. After incubation for 15 min on ice, the cells were washed twice with ice-cold PBS, and then serum-free RPMI 1640 containing both goat pAbs to rat IgG (20 μg/ml) (Jackson ImmunoResearch) and glutaraldehyde-stabilized IgG-opsonized sheep RBCs (Ig-sRBCs) (5×10^7 per well) (Inter-Cell Technologies) was added. IgG-opsonized, non-opsonized, or C3bi-opsonized mouse RBCs were also tested by the same procedure. After incubation for 15 min on ice, culture plates were transferred to a water bath at 37 °C to initiate phagocytosis. Phagocytosis was terminated after the indicated times by again placing the plates on ice, and the cells were washed with ice-cold PBS three times. The PEMs were then fixed with 4% paraformaldehyde in PBS, after which phagocytosed RBCs were detected with a phase-contrast microscope, and random fields were photographed. For phagocytosis assays with mouse RBCs, the PEMs were incubated for 5 min at room temperature with hemolysis buffer (154 mM NH_4Cl (pH 7.3), 10 mM $KHCO_3$, 0.1 mM EDTA) before fixation to remove attached RBCs. To determine the phagocytosis index, we identified >100 cells in randomly chosen fields of view, and the percentage of cells that had engulfed RBCs was determined. For characterization of signaling downstream of SIRPβ, PEMs were treated with mAbs to SIRPβ and secondary cross-linking antibodies as described above. Cell lysates were then prepared and subjected to immunoprecipitation and immunoblot analysis.

Immunocytofluorescence—PEMs were fixed for 20–30 min at room temperature in PBS containing 4% paraformaldehyde and 0.1% glutaraldehyde and were then permeabilized for 60 min at room temperature in PBS containing 0.1% Triton X-100 and 5% goat serum (blocking solution). After incubation for 1 h at room temperature or overnight at 4 °C with primary antibodies diluted in blocking solution, the cells were washed with PBS and incubated for 1 h at room temperature with Alexa488-conjugated secondary antibodies (Molecular Probes) diluted in blocking solution. For visualization of F-actin, cells were incubated with rhodamine-conjugated phalloidin (Molecular Probes) together with the secondary antibodies. The cells were finally washed with PBS and mounted. Fluorescence images were acquired with a laser-scanning confocal microscope (LSM5 PASCAL, Zeiss).

RESULTS

Cloning of Mouse SIRPβ cDNAs and Tissue Distribution of SIRPβ mRNA—To investigate the role of SIRPβ in macrophage function, we first cloned mouse SIRPβ cDNAs. A data base search based on the homology between human and mouse SIRPβ cDNAs yielded two mouse EST clones (BB637627 and BB666974 (DDBJ)) that correspond to the 5′ region of SIRPβ cDNA (~0.7 kb), including the initiation codon, as well as two EST clones (BB144964 and BB559616 (DDBJ)) corresponding to the 3′ region of SIRPβ cDNA (~0.7 kb), including the termination codon. We designed PCR primers based on the sequences of these EST clones to isolate a full-length SIRPβ cDNA (DDBJ accession number AB112022) by PCR from a C57BL/6 mouse spleen cDNA library. We also cloned another full-length SIRPβ cDNA (DDBJ accession number AB112024) from a Balb/c mouse spleen cDNA library by RACE-PCR. These C57BL/6 and Balb/c mouse cDNAs comprise 1317 and 1232 bp, respectively, and each contain a single open reading frame (1173 bp) that encodes a protein of 391 amino acids (Fig. 1*A*).

The predicted structure of mouse SIRPβ is similar to that of the human protein (11); it is a putative transmembrane protein with three Ig-like domains in its extracellular region and a short cytoplasmic tail (Fig. 1, *A* and *B*). The first Ig domain is homologous to a V-type Ig domain, whereas the second and third Ig domains resemble a C1-type Ig domain (33). The overall amino acid sequence identity between the C57BL/6 and Balb/c SIRPβ proteins is 94.4% (22 residue differences) (Fig. 1*B*), suggesting that the SIRPβ gene is polymorphic among mouse strains. The sequence differences between the two mouse SIRPβ isoforms are concentrated in the first Ig domain (amino acids 29–144), which exhibits a sequence identity of 89% (Fig. 1*B*). We also cloned partial cDNAs from C57BL/6 and Balb/c mouse spleen (DDBJ accession numbers AB112023 and AB112025, respectively) that are homologous to but significantly different from the corresponding full-length SIRPβ cDNAs (data not shown).

Although human SIRPβ has been shown to be expressed in myeloid cells, including monocytes and dendritic cells, but not in lymphocytes (12), its tissue distribution was otherwise unknown. RT-PCR analysis revealed that mouse SIRPβ mRNA is most abundant in brain, spleen, kidney, and testis but is also present in smaller amounts in other tissues (Fig. 1*C*). We also confirmed the presence of SIRPβ mRNA in macrophage lineage cells, including thioglycolate-elicited mouse PEMs and mouse RAW264.7 macrophages (Fig. 1*D*).

Promotion of Phagocytosis in Macrophages by mAb Engagement of SIRPβ—To examine the possible role of SIRPβ in phagocytosis by macrophages, we generated several rat mAbs to the extracellular region of SIRPβ with the use of an SIRPβ-Fc fusion protein (the extracellular portion of mouse SIRPβ fused to the Fc portion of human IgG) as an antigen. From these mAbs, we chose mAb 80 and mAb 84 for the following experiments. We also generated rabbit polyclonal antibodies to SIRPβ with the same SIRPβ-Fc fusion protein as antigen. Immunoblot analysis revealed that the pAbs to SIRPβ reacted with mouse SIRPβ or mouse SHPS-1 expressed in CHO-Ras cells (CHO cells transformed as a result of expression of an active form of H-Ras) (Fig. 2*A*). This cross-reactivity was not unexpected given that the amino acid sequences of the extracellular regions of mouse SIRPβ and SHPS-1 are 65% identical. In contrast, both mAb 80 and mAb 84 reacted with SIRPβ but not with SHPS-1 (Fig. 2*A*), indicating that these antibodies are specific for SIRPβ. Two distinct immunoreactive bands corresponding to SIRPβ (~90 and 60 kDa) were observed in CHO-Ras transfectants (Fig. 2*A*); these two bands migrated as a single protein of ~40 kDa after treatment of total cell

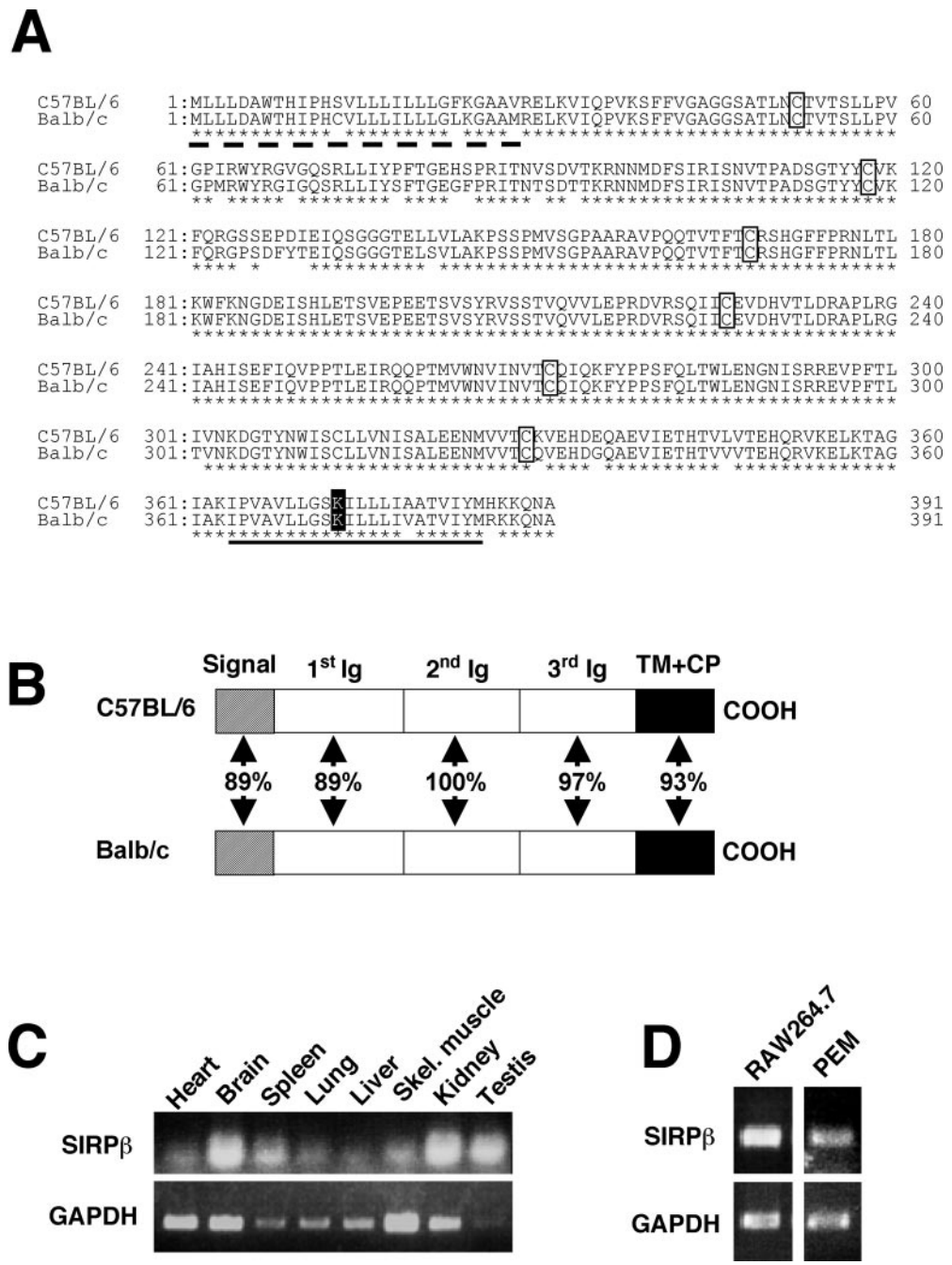

FIG. 1. **Structure of mouse SIRPβ and tissue distribution of its mRNA.** *A*, deduced amino acid sequences of C57BL/6 and Balb/c mouse SIRPβ. *Asterisks* indicate identical residues; the *dotted line* denotes the predicted NH_2-terminal signal sequence; cysteine residues that likely form disulfide bonds in the three Ig-like domains are *boxed*; the predicted transmembrane region is *underlined*; and a lysine residue that might interact with an aspartic acid residue of DAP12 is *highlighted*. The nucleotide sequences of C57BL/6 and Balb/c mouse SIRPβ cDNAs have been submitted to the DDBJ with accession numbers AB112022 and AB112024, respectively. *B*, homology between C57BL/6 and Balb/c mouse SIRPβ proteins. The putative signal sequence, three Ig-like domains, and combined transmembrane region and short cytoplasmic tail (*TM + CP*) are represented by *boxes*. The sequence identity between these corresponding regions of the two proteins is indicated. *C* and *D*, RT-PCR analysis of the distribution of SIRPβ mRNA among various mouse tissues (*C*) as well as mouse PEMs and RAW264.7 cells (*D*). The positions of RT-PCR products corresponding to SIRPβ and glyceraldehyde-3-phosphate dehydrogenase (*GAPDH*) mRNAs are indicated.

lysates with *N*-glycosidase-F (data not shown), suggesting that they corresponded to two distinct glycosylated forms of SIRPβ. Immunoblot analysis with mAb 80 of immunoprecipitates prepared from mouse PEMs with the pAbs to SIRPβ yielded a broad band (~50–70 kDa) corresponding to SIRPβ (Fig. 2*B*), confirming that SIRPβ mRNA is translated into protein in these cells.

We then tested the effects of the mAbs to SIRPβ on the phagocytosis of Ig-sRBCs by thioglycolate-elicited mouse PEMs or RAW264.7 cells *in vitro*. Either mAb 80 or mAb 84 alone induced only a small increase in the extent of phagocytosis by PEMs, compared with that apparent with an isotype-matched control rat IgG (Fig. 3*A*). In contrast, cross-linking of these mAbs by secondary antibodies markedly increased the phagocytosis of Ig-sRBCs by PEMs; this effect was dependent both on the time of incubation (maximal at 5–10 min) and on the concentration of mAb (maximal at 20 μg/ml) (data not shown). We found that cross-linking of control rat IgG by secondary antibodies induced a significant decrease (~30%) in phagocytic activity, as compared with that observed without any treat-

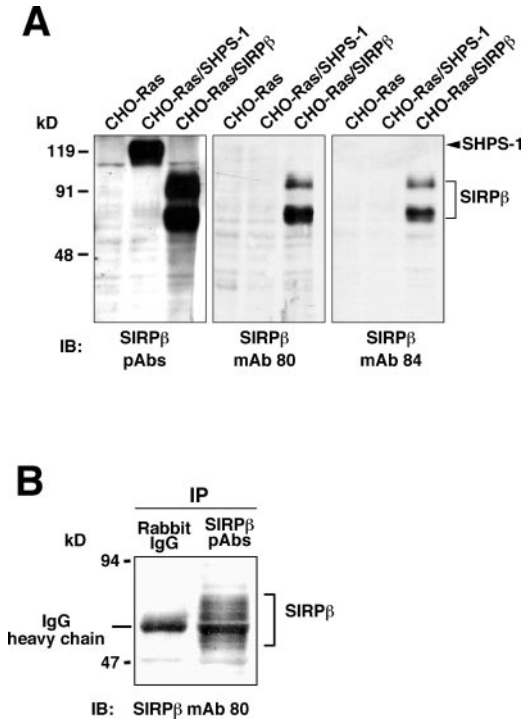

FIG. 2. **Characterization of antibodies to SIRPβ and expression of SIRPβ in PEMs.** *A*, CHO-Ras cells and CHO-Ras cells expressing either mouse SHPS-1 (*CHO-Ras/SHPS-1* cells) or mouse SIRPβ (*CHO-Ras/SIRPβ* cells) were lysed and subjected to immunoblot analysis (*IB*) with pAbs, mAb 80, or mAb 84 to SIRPβ as indicated. The positions of SHPS-1 and SIRPβ and those of molecular size standards are indicated. *B*, lysates of mouse PEMs were subjected to immunoprecipitation (*IP*) with pAbs to SIRPβ (or with normal rabbit IgG as a control), and the resulting precipitates were subjected to immunoblot analysis with mAb 80. The positions of SIRPβ and IgG heavy chain as well as those of molecular size standards are indicated.

ment (data not shown). It might be mediated through the stimulation of FcγRII by the cross-linking. Even if there were such inhibition on phagocytosis by addition of antibodies, the promotion of phagocytosis by specific mAbs to SIRPβ was specific and significant. Similar results were obtained with RAW264.7 cells instead of PEMs (Fig. 3*B*). Cross-linking of mAbs to SIRPβ also promoted the phagocytosis by PEMs of IgG-opsonized mouse RBCs and, to a lesser extent, that of non-opsonized mouse RBCs (Fig. 3*C*). Ligation of complement receptors also promoted phagocytosis by macrophages (9), and cross-linking of mAbs to SIRPβ increased the phagocytosis of C3bi-opsonized mouse RBCs by PEMs (Fig. 3*D*). These results suggest that engagement of SIRPβ by specific mAbs promoted FcγR-dependent or FcγR-independent phagocytosis by macrophages and that this effect might be mediated, at least in part, by a signaling pathway distinct from that activated by FcγR or the complement receptor.

Roles of MAPK and MEK in the Promotion of Phagocytosis by Ligation of SIRPβ—Activation of the PI 3-kinase signaling pathway is implicated in FcγR-stimulated phagocytosis (7, 34, 35). The contribution of MAPK to FcγR-stimulated phagocytosis, however, is controversial (36, 37). We therefore next examined whether engagement of SIRPβ induces activation of MAPK or of Akt, the latter of which functions downstream of PI 3-kinase (38). M-CSF activates both MAPK and PI 3-kinase pathways in macrophages (39). In the present study, M-CSF also induced marked activation of MAPK in PEMs (Fig. 4*A*). Engagement of SIRPβ by either mAb 80 or mAb 84 also triggered marked activation of MAPK. In addition, activation of the upstream kinase MEK was observed in response either to M-CSF or to ligation of SIRPβ by mAbs 80 or 84. However, whereas M-CSF induced marked activation of Akt in PEMs, engagement of SIRPβ by either mAb triggered weak activation of Akt (Fig. 4*A*).

To examine whether the activation of MEK and MAPK induced by the engagement of SIRPβ contributes to the promotion of phagocytosis by SIRPβ, we investigated the effects of two different MEK inhibitors, PD98059 (40) and U0126 (41). Treatment of PEMs with either PD98059 (Fig. 4*B*) or U0126 (Fig. 4*C*) prevented the stimulatory effect of mAbs to SIRPβ on FcγR-mediated phagocytosis but had no effect on the basal level of such phagocytosis observed in the presence of control rat IgG. Both MEK inhibitors also abolished the activation of MAPK elicited by engagement of SIRPβ as well as the basal activation of this kinase apparent in the presence of control rat IgG (Fig. 4, *B* and *C*). These data thus suggest that activation of the MEK-MAPK pathway contributes to the promotion of FcγR-mediated phagocytosis induced by engagement of SIRPβ. In contrast, this pathway does not appear to contribute to the basal level of FcγR-mediated phagocytosis, consistent with the results of Karimi and Lennartz (36).

Wortmannin, an inhibitor of PI 3-kinase (42), partially inhibited both the stimulatory effect of SIRPβ ligation on FcγR-mediated phagocytosis as well as the basal level of such phagocytosis in PEMs (Fig. 4*D*). However, the promotion of phagocytosis induced by engagement of SIRPβ was still observed in the presence of wortmannin. We confirmed that wortmannin abolished the activation of Akt by M-CSF or by engagement of SIRPβ in these cells. These results are thus consistent with the notion that the activation of PI 3-kinase contributes to FcγR-stimulated phagocytosis (7, 34, 35). However, the activation of PI 3-kinase does not appear to contribute substantially to the promotion of FcγR-mediated phagocytosis by engagement of SIRPβ.

Role of Myosin Light Chain Kinase (MLCK) in the Promotion of Phagocytosis by Ligation of SIRPβ—Activation of MLCK by MAPK is implicated in the positive regulation of cell adhesion and cell migration mediated by cytoskeletal reorganization (43, 44). Given that our results suggested that the MEK-MAPK pathway is important for the promotion of phagocytosis by engagement of SIRPβ, we next examined the effects on this process of ML-7, chemical inhibitors of MLCK (45, 46). ML-7 completely blocked the stimulatory effect of SIRPβ engagement on FcγR-mediated phagocytosis (Fig. 5*A*); it also slightly inhibited the basal level of such phagocytosis observed in the presence of control rat IgG. We confirmed the inhibitory effect of ML-7 on MLCK in GbaSM-4 cells, a vascular smooth muscle cell line derived from brain basilar arteries. SPC induced phosphorylation of MLC in GbaSM-4 cells (Fig. 5*B*) as described previously (47). ML-7 completely blocked the SPC-induced phosphorylation of MLC in GbaSM-4 cells (Fig. 5*B*). Activated MLCK could phosphorylate MLC and activate the myosin ATPase activity. Chemical inhibitor of the ATPase activity of myosin, BDM (46, 48), also prevented the promotion of FcγR-mediated phagocytosis by SIRPβ ligation as well as significantly inhibited the basal level of such phagocytosis (Fig. 5*C*). These observations thus suggest that the activation of MLCK contributes to the promotion of phagocytosis by engagement of SIRPβ probably through the activation of myosin ATPase activity.

Effects of SIRPβ Engagement on the Actin Cytoskeleton and on the Localization of Activated MAPK—Reorganization of the actin cytoskeleton is essential for phagocytosis by macrophages (8, 49). We therefore next examined the effects of engagement of SIRPβ on the actin cytoskeleton and on the localization of activated MAPK. Immunofluorescence analysis with rhodamine-conjugated phalloidin revealed that PEMs treated with

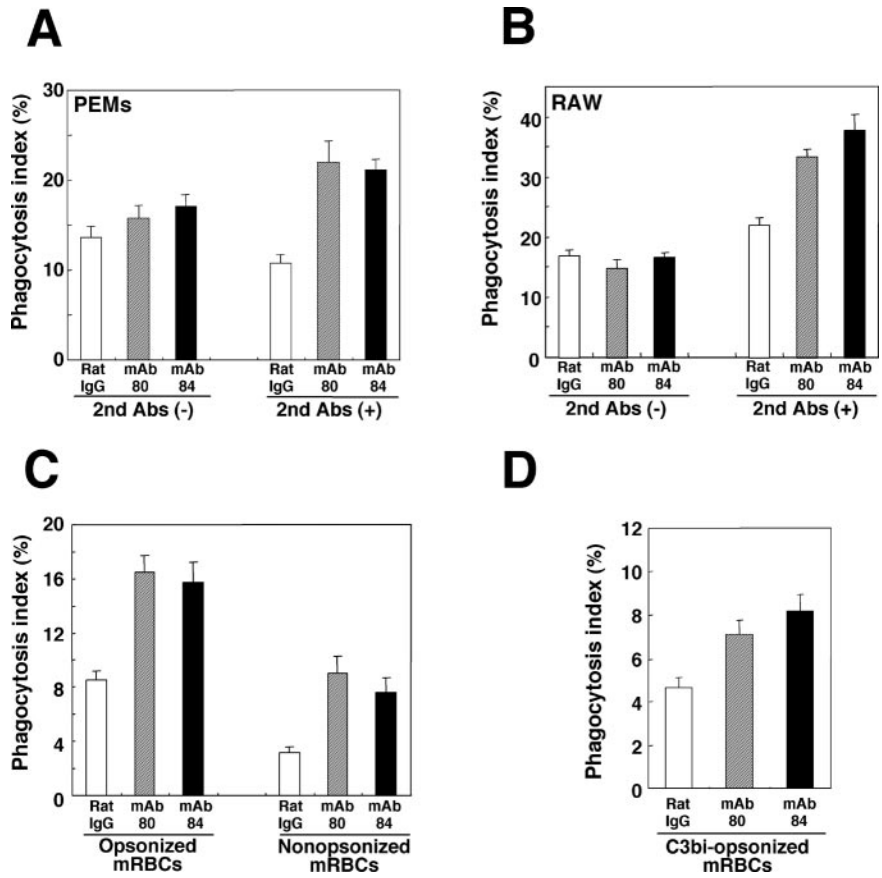

FIG. 3. **Phagocytosis by macrophages in response to cross-linking of mAbs to SIRPβ.** *A*, primary cultured PEMs were incubated on ice with mAbs 80 or 84 to SIRPβ (or with isotype-matched control rat IgG) before the addition of Ig-sRBCs in the absence or presence of secondary cross-linking antibodies (*2nd Abs*). After incubation for 5 min at 37 °C, the PEMs were fixed, and the extent of phagocytosis was determined. *B*, RAW264.7 cells were treated as described in *A* with the exception that the incubation at 37 °C was performed for 20 min. *C*, PEMs were treated as in *A* with the exception that the incubation at 37 °C was performed in the presence of secondary antibodies either for 15 min with IgG-opsonized mouse RBCs (*mRBCs*) or for 120 min with non-opsonized mouse RBCs. *D*, PEMs were treated as in *A* with the exception that the incubation at 37 °C was performed for 60 min in the presence of secondary antibodies and C3bi-opsonized mouse RBCs. All data are means ± S.E. of values from 10 different fields of view and are representative of three separate experiments.

control rat IgG exhibited a few scattered filopodia at the cell periphery (Fig. 6*A*). Immunostaining also revealed that activated MAPK was localized predominantly to the nucleus and perinuclear region of control IgG-treated PEMs. Engagement of SIRPβ by either mAb 80 or mAb 84 induced the formation of prominent filopodia and lamellipodia, many of which protruded focally at the cell periphery, as well as caused the cells to adopt an elongated morphology. In addition to its presence in the nucleus, activated MAPK also became localized both at the cell periphery, including the sites of filopodia and lamellipodia, as well as in the cytoplasm of PEMs treated with the mAbs. The formation of filopodia and lamellipodia as well as the induction of an elongated cell morphology and the redistribution of activated MAPK observed in response to engagement of SIRPβ were markedly inhibited by treatment of PEMs with either PD98059 or ML-7 but not by that with wortmannin (Fig. 6*B*).

Roles of DAP12 and Syk in the Promotion of Phagocytosis by SIRPβ Engagement—SIRPβ forms a complex with DAP12 and engagement of SIRPβ induces tyrosine phosphorylation of DAP12 and its subsequent association with the tyrosine kinase Syk in cells overexpressing SIRPβ and DAP12 (13, 14). We found that DAP12 was coimmunoprecipitated with SIRPβ from PEMs (Fig. 7*A*), suggesting that the two proteins also form a complex in these cells. Engagement of SIRPβ by either mAb 80 (data not shown) or mAb 84 (Fig. 7*B*) markedly stimulated the tyrosine phosphorylation of DAP12 as well as its association with Syk. Engagement of SIRPβ also substantially increased the tyrosine phosphorylation of Syk (Fig. 7*C*), suggesting that SIRPβ ligation results in the activation of Syk.

To examine further the possible role of Syk in the stimulation of FcγR-mediated phagocytosis by SIRPβ ligation, we tested the effect of the Syk inhibitor piceatannol (50) on this process. Piceatannol prevented the promotion of FcγR-mediated phagocytosis induced by engagement of SIRPβ (Fig. 7*D*). Piceatannol also inhibited the tyrosine phosphorylation of Syk induced by mAbs 80 or 84 (Fig. 7*E*). Furthermore, piceatannol abolished the activation of MAPK induced by engagement of SIRPβ (Fig. 7*F*). We also examined the effect of a dominant-negative mutant of Syk on the promotion of FcγR-mediated phagocytosis induced by SIRPβ engagement. To this end, RAW264.7 cells were cotransfected with vectors for GFP and kinase-negative Syk (51) and thereafter subjected to phagocytosis assay. Expression of kinase-negative Syk markedly inhibited the promotion of FcγR-mediated phagocytosis induced by SIRPβ engagement (Fig. 7*G*). These results thus suggest that engagement of SIRPβ promotes phagocytosis through tyrosine phosphorylation of DAP12, the subsequent association of DAP12 with Syk, and the consecutive activation of Syk and MAPK.

Effects of SIRPβ Engagement on the Tyrosine Phosphorylation of SLP-76 and BLNK—Syk and the related tyrosine kinase ZAP-70 phosphorylate the adapter protein SLP-76 (52–54). In addition, both SLP-76 and BLNK, another adapter protein, are expressed in bone marrow-derived macrophages (55). We therefore examined the effect of engagement of SIRPβ on the tyrosine phosphorylation of SLP-76 and BLNK in PEMs. Ligation of SIRPβ by either mAb 80 or mAb 84 markedly increased the tyrosine phosphorylation of SLP-76 (Fig. 8*A*), and this effect was blocked by piceatannol (Fig. 8*B*). In contrast, ligation of SIRPβ did not affect the tyrosine phosphorylation of BLNK (Fig. 8*C*). Our results thus implicate SLP-76 as an adapter protein that functions downstream of Syk in PEMs activated by engagement of SIRPβ.

DISCUSSION

We have cloned mouse SIRPβ cDNAs and thereby shown that the overall structure of the encoded proteins is similar to that of human SIRPβ. We also found that the amino acid

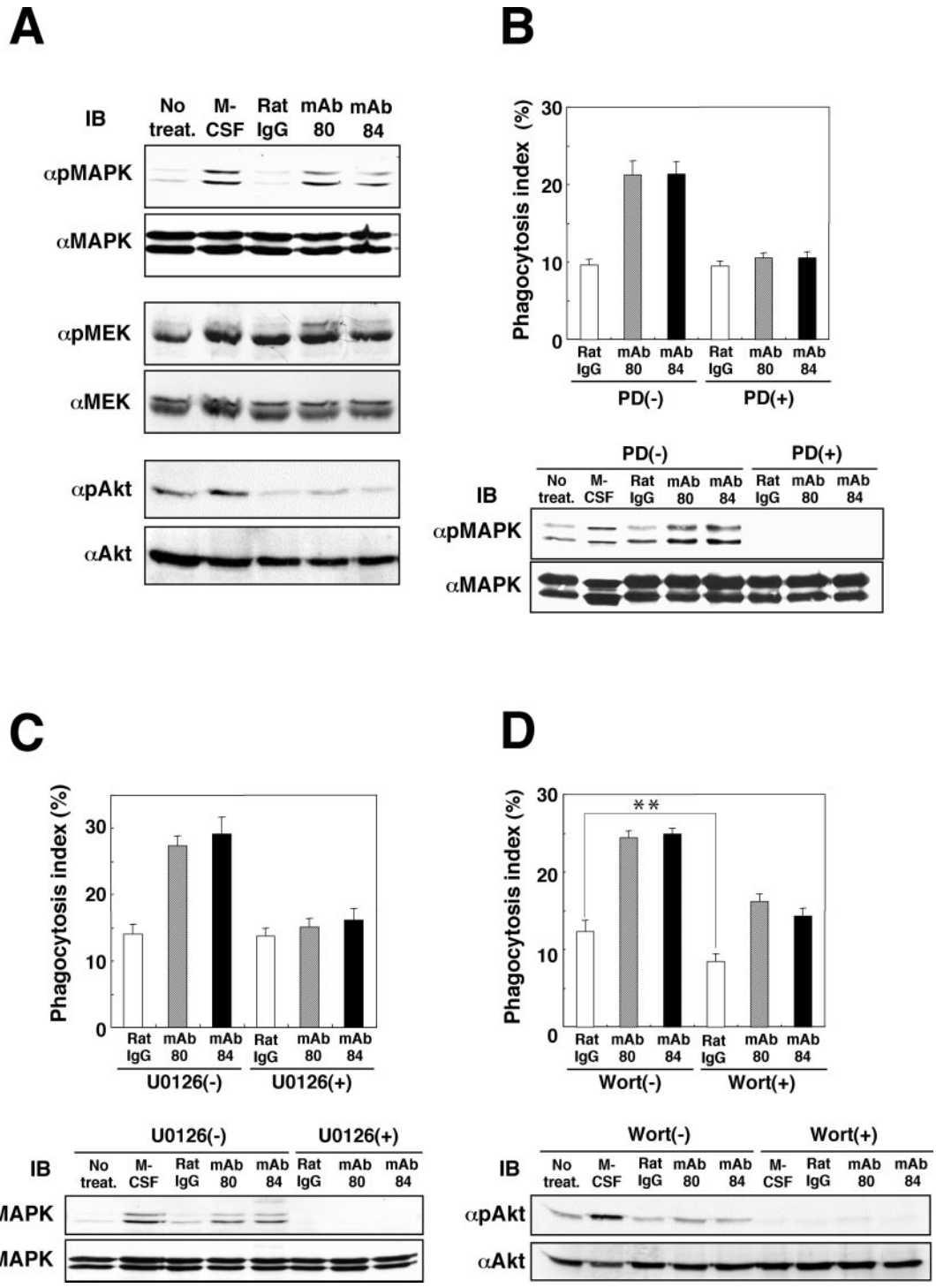

FIG. 4. **Roles of MAPK and MEK in the promotion of FcγR-mediated phagocytosis by ligation of SIRPβ in PEMs.** *A*, PEMs treated with mAbs to SIRPβ (or isotype-matched control rat IgG) and with secondary cross-linking antibodies as described under "Experimental Procedures" were incubated for 10 min at 37 °C. As positive and negative controls, PEMs were incubated for 5 min at 37 °C with M-CSF (10 ng/ml) or were left untreated, respectively. The cells were then lysed and subjected to immunoblot (*IB*) analysis with pAbs to active forms of MAPK (*αpMAPK*), MEK (*αpMEK*), or Akt (*αpAkt*); duplicate samples were also analyzed with pAbs to MAPK (*αMAPK*), MEK (*αMEK*), or Akt (*αAkt*). *B–D*, PEMs were incubated for 30 min at 37 °C in the absence or presence of 50 μM PD98059 (*PD*) (*B*), 2 μM U0126 (*C*), or 100 nM wortmannin (*Wort*) (*D*) before treatment with mAbs to SIRPβ (or control rat IgG) and secondary cross-linking antibodies (in the continued absence or presence of inhibitor) as described in *A*. After incubation for 5 min at 37 °C with Ig-sRBCs, the cells were fixed, and the extent of phagocytosis was determined (*upper panels*). Alternatively, PEMs were incubated in the absence or presence of inhibitors, treated with mAbs to SIRPβ and secondary cross-linking antibodies, and incubated for 10 min at 37 °C. The cells were then lysed and subjected to immunoblot analysis with pAbs to active forms of MAPK (*B* and *C*) or Akt (*D*); duplicate samples were also analyzed with pAbs to MAPK or to Akt (*lower panels*). Positive and negative controls were as in *A*. Data for phagocytosis assays are means ± S.E. of values from 10 different fields of view; **, $p < 0.01$ for the indicated comparison (Student's *t* test). All results are representative of three separate experiments.

sequence of mouse SIRPβ differs between the C57BL/6 and Balb/c strains, with the residue differences being concentrated in the NH_2-terminal V-type Ig domain in the extracellular region of the protein. Nucleotide and amino acid substitutions were also previously identified in the extracellular region of SHPS-1 from different mouse strains (56). It is possible that

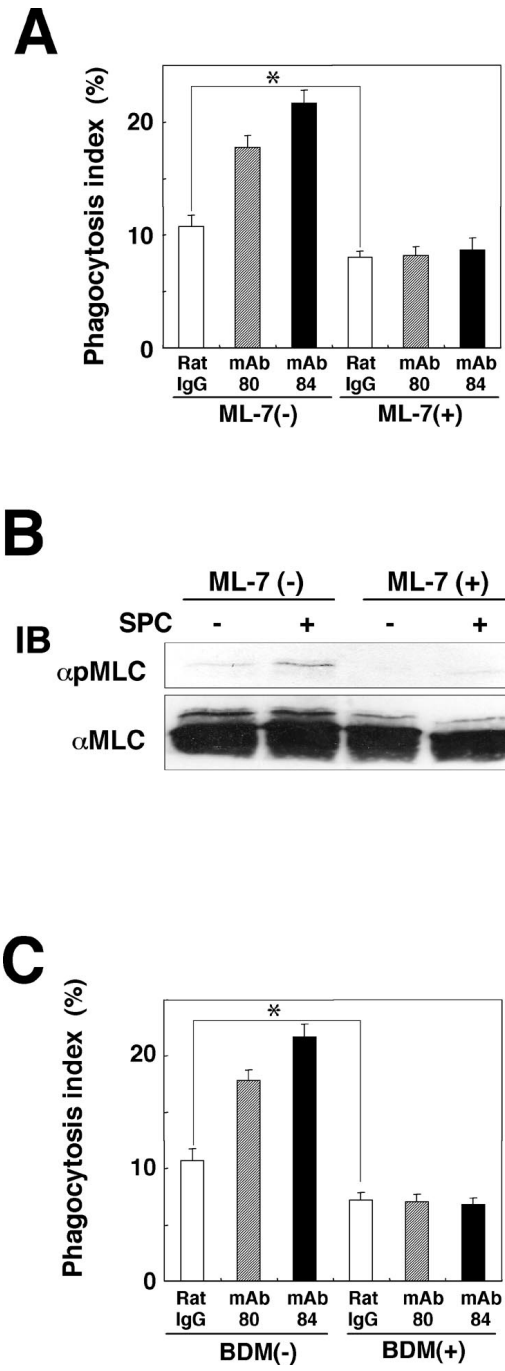

FIG. 5. **Role of MLCK in the promotion of phagocytosis by SIRPβ engagement in PEMs.** *A*, PEMs were incubated for 30 min at 37 °C in the absence or presence of 10 μM ML-7 before treatment with mAbs to SIRPβ (or control rat IgG) and secondary cross-linking antibodies (in the continued absence or presence of inhibitor). After incubation for 5 min at 37 °C with Ig-sRBCs, the cells were fixed, and the extent of phagocytosis was determined. *B*, serum-deprived GbaSM-4 cells were incubated for 30 min at 37 °C in the absence or presence of 10 μM ML-7 and further incubated with 1 μM SPC for 2 min at 37 °C. The cells were then treated with ice-cold trichloroacetic acid to precipitate total cellular proteins. The precipitated proteins were subjected to immunoblot (*IB*) analysis with pAbs to phosphorylated forms of MLC (*αpMLC*). Duplicated samples were also analyzed by immunoblot analysis with a mAb to MLC (*αMLC*). *C*, PEMs were incubated for 30 min at 37 °C in the absence or presence of 50 mM BDM before treatment with mAbs to SIRPβ (or control rat IgG) and secondary cross-linking antibodies (in the continued absence or presence of inhibitor). After incubation for 5 min at 37 °C with Ig-sRBCs, the cells were fixed, and the extent of phagocytosis was determined. All phagocytosis data are means ± S.E. of values from 10 different fields of view; *, $p < 0.05$ for the indicated comparisons (Student's *t* test). All results are representative of three separate experiments.

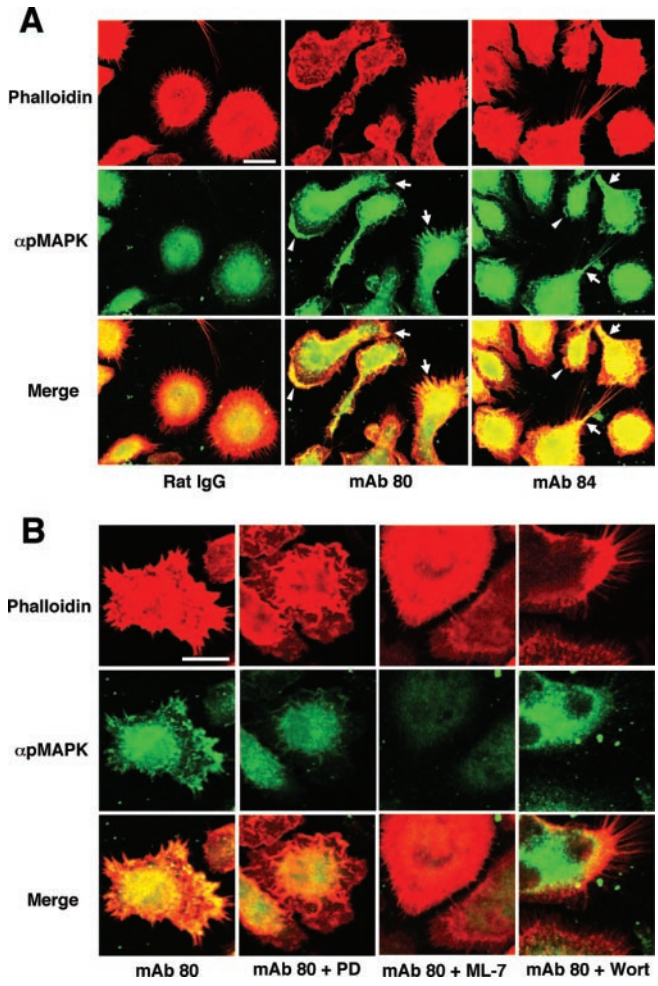

FIG. 6. **Reorganization of the actin cytoskeleton and redistribution of activated MAPK induced by SIRPβ engagement in PEMs.** *A*, PEMs were treated with mAbs 80 or 84 to SIRPβ (or isotype-matched control rat IgG) and with secondary cross-linking antibodies as described under "Experimental Procedures." After incubation for 5 min at 37 °C, the cells were fixed and stained with both rhodamine-conjugated phalloidin (*red*) and pAbs to activated MAPK (*green*). Merged images are also shown. *Arrows* and *arrowheads* indicate immunoreactivity of activated MAPK at sites of filopodia and lamellipodia, respectively. *B*, PEMs were incubated for 30 min at 37 °C in the absence or presence of 50 μM PD98059, 10 μM ML-7, or 100 nM wortmannin (*Wort*) before treatment with mAb 80 to SIRPβ and secondary cross-linking antibodies (in the continued absence or presence of inhibitor). After incubation for 5 min at 37 °C, the cells were fixed and stained as in *A*. *Scale bars*, 20 μm. All results are representative of three separate experiments.

the heterogeneity of amino acid sequence in the extracellular region of SIRPβ might result in heterogeneous biological responses to the putative ligand of this protein. SIRPβ was shown previously to be expressed in hematopoietic cells (12, 13, 14). We have now shown that SIRPβ mRNA is present in the spleen and macrophages but also in other organs including the brain, kidney, and testis. SIRPβ might thus play multiple roles in various tissues or cell types.

We generated mAbs that recognize SIRPβ but not SHPS-1. With the use of these antibodies, we showed that SIRPβ is indeed expressed in PEMs as well as that engagement of SIRPβ by the mAbs promotes FcγR-mediated phagocytosis by either PEMs or RAW264.7 cells. Engagement of SIRPβ also promoted both the phagocytosis of non-opsonized mouse RBCs and complement receptor-mediated phagocytosis. SIRPβ thus appears to be a new member of the group of transmembrane proteins that promote phagocytosis in macrophages, at least in part,

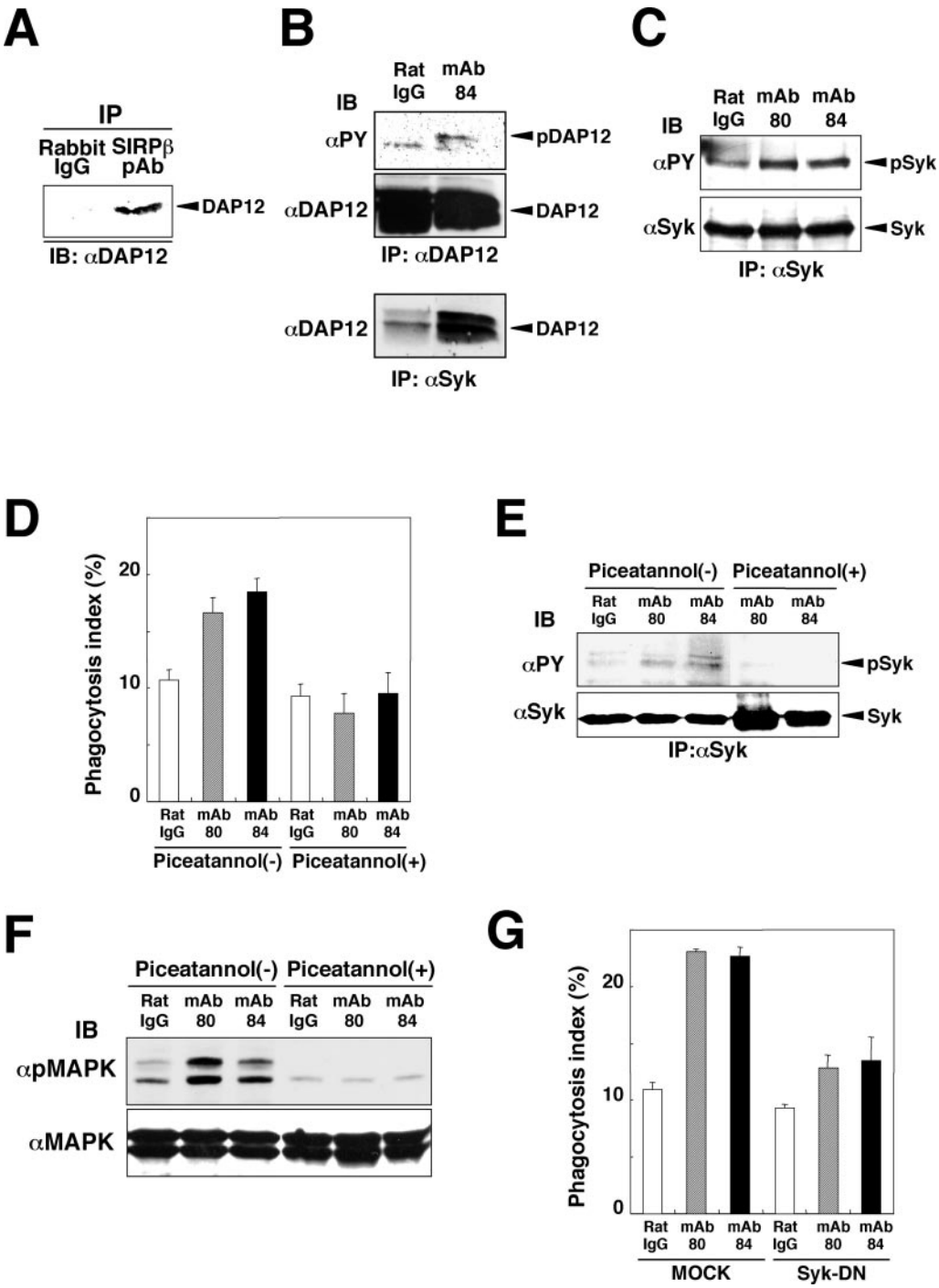

FIG. 7. **Roles of DAP12 and Syk in the promotion of phagocytosis by engagement of SIRPβ.** *A*, PEM lysates were subjected to immunoprecipitation (*IP*) with pAbs to SIRPβ (or with normal rabbit IgG), and the resulting precipitates were subjected to immunoblot (*IB*) analysis with pAbs to DAP12 (*αDAP12*). The position of DAP12 is indicated. *B*, PEMs were treated with mAb 84 (or isotype-matched control rat IgG) and secondary cross-linking antibodies as described under "Experimental Procedures." After incubation for 5 min at 37 °C, cell lysates were prepared and subjected to immunoprecipitation with pAbs to DAP12. The resulting precipitates were subjected to immunoblot analysis with a mAb to phosphotyrosine (*αPY*); duplicate samples were also analyzed with pAbs to DAP12. The positions of phosphorylated DAP12 (*pDAP12*) and total DAP12 are indicated (*upper panels*). The PEM lysates were also subjected to immunoprecipitation with pAbs to Syk (*αSyk*) and subsequent immunoblot analysis with pAbs to DAP12 (*lower panel*). *C*, PEMs were treated with mAbs to SIRPβ and secondary cross-linking antibodies as described in *B*, after which cell lysates were subjected to immunoprecipitation with pAbs to Syk and subsequent immunoblot analysis with a mAb to phosphotyrosine. Duplicate immunoprecipitates were also subjected to immunoblot analysis with pAbs to Syk. The positions of phosphorylated Syk (*pSyk*) and total Syk are indicated. *D*, PEMs were incubated for 30 min at 37 °C in the absence or presence of 10 μM piceatannol before treatment with mAbs to SIRPβ and secondary cross-linking antibodies (in the continued absence or presence of piceatannol). After incubation for 5 min at 37 °C with Ig-sRBCs, PEMs were fixed, and the extent of phagocytosis was determined. Data are means ± S.E. of values from 10 different fields of view. *E* and *F*, PEMs treated with piceatannol, mAbs to SIRPβ, and secondary cross-linking antibodies as in *D* were lysed and subjected to immunoprecipitation with pAbs to Syk and subsequent immunoblot analysis with either a mAb to phosphotyrosine or pAbs to Syk (*E*). Alternatively, the cell lysates were subjected to immunoblot analysis with pAbs either to active MAPK or to MAPK (*F*). *G*, RAW264.7 cells were cotransfected with vectors for GFP and kinase-negative Syk (*Syk-DN*) or the corresponding empty vector (*MOCK*). Twenty four h after transfection, cells were incubated with mAbs to SIRPβ (or isotype-matched control rat IgG) and with secondary cross-linking antibodies. After incubation with Ig-sRBCs for 20 min at 37 °C, cells were fixed, and the extent of phagocytosis of the cells expressing GFP was determined. Data are means ± S.E. of values from 10 different fields of view. All results are representative of three separate experiments.

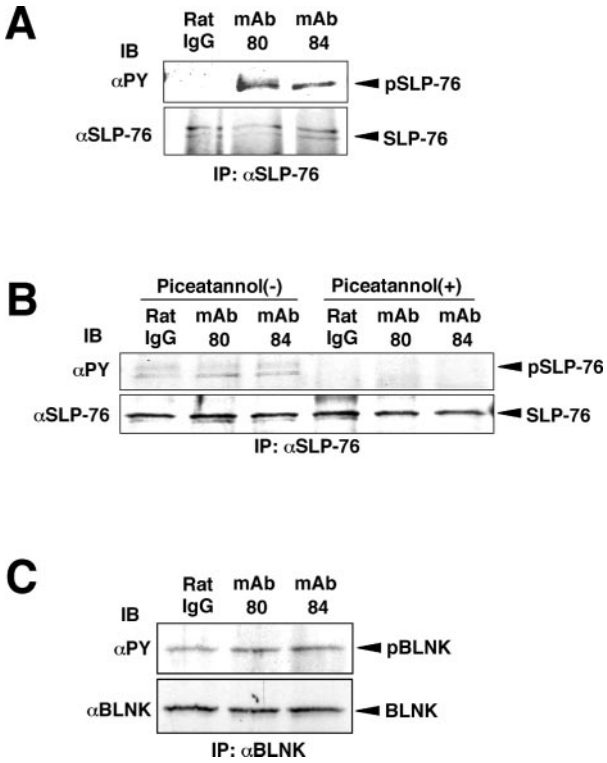

FIG. 8. **Tyrosine phosphorylation of SLP-76, but not of BLNK, in response to engagement of SIRPβ in PEMs.** *A* and *C*, PEMs were treated with mAbs to SIRPβ and secondary cross-linking antibodies as described under "Experimental Procedures." After incubation for 10 min at 37 °C, the cells were lysed and subjected to immunoprecipitation (*IP*) with pAbs to SLP-76 (*αSLP-76*) (*A*) or to BLNK(*αBLNK*) (*C*). The resulting precipitates were subjected to immunoblot (*IB*) analysis with a mAb to phosphotyrosine or with pAbs to SLP-76 (*A*) or to BLNK (*C*). The positions of phosphorylated or total SLP-76 and BLNK are indicated. *B*, PEMs were incubated for 30 min at 37 °C in the absence or presence of 10 μM piceatannol before treatment with mAbs to SIRPβ and secondary cross-linking antibodies (in the continued absence or presence of piceatannol). After incubation for 5 min at 37 °C, the cells were lysed and subjected to immunoprecipitation with pAbs to SLP-76 and subsequent immunoblot analysis with a mAb to phosphotyrosine; duplicate precipitates were also subjected to immunoblot analysis with pAbs to SLP-76. All results are representative of three separate experiments.

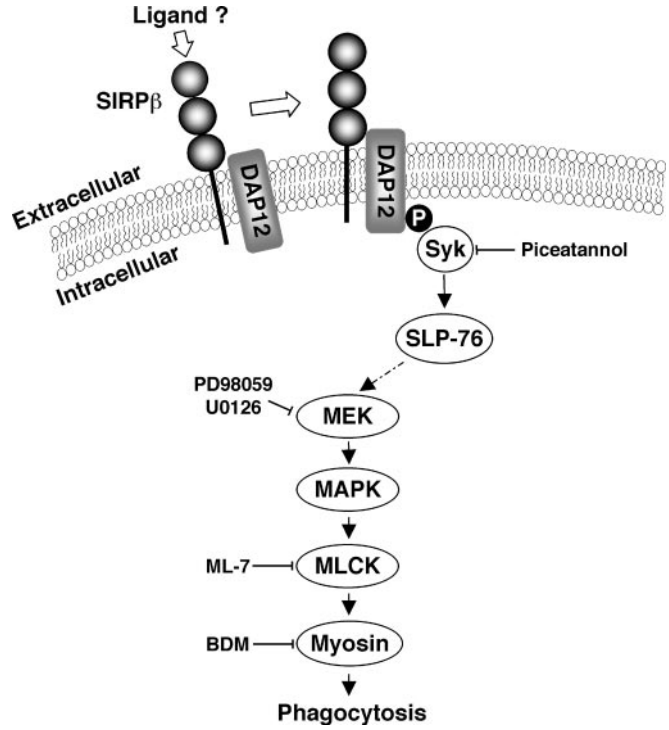

FIG. 9. **Proposed model for the signaling pathway that underlies the promotion of phagocytosis by SIRPβ in macrophages.** See text for details.

through the activation of a signaling pathway distinct from that triggered by FcγR or the complement receptor.

We also investigated the signaling pathway activated by engagement of SIRPβ in PEMs. Ligation of SIRPβ by specific mAbs induced marked activation of MEK and MAPK, and it also induced weak activation of Akt. The SIRPβ-promoted phagocytic response was markedly blocked by inhibitors of MEK but not by the PI 3-kinase inhibitor wortmannin. Engagement of SIRPβ also induced the formation of prominent filopodia and lamellipodia as well as caused PEMs to adopt an elongated morphology. It also induced the recruitment of active MAPK to sites near these filopodia and lamellipodia. These effects were markedly inhibited by a MEK inhibitor but not by wortmannin. Moreover, we showed that inhibitors of MLCK and of myosin ATPase each blocked the promotion of phagocytosis by SIRPβ ligation. The activation of MAPK was shown previously to stimulate MLCK activity and thereby to promote cell adhesion and migration through reorganization of the actin cytoskeleton in COS cells and REF52 fibroblasts (43, 44). The activated MAPK was also recruited to the sites of newly formed focal adhesions, and this response was blocked by inhibitors of MEK or MLCK (44). We also found that recruitment of active MAPK to the cell periphery induced by SIRPβ ligation was blocked by an MLCK inhibitor. In macrophages, activated MAPK is thought to trigger the activation of MLCK through direct phosphorylation (37). Together, our present results thus suggest that engagement of SIRPβ promotes phagocytosis through activation of a MEK-MAPK-MLCK pathway and subsequent reorganization of the actin cytoskeleton.

SIRPβ was shown previously to bind DAP12 (13, 14). Furthermore, engagement of SIRPβ resulted in the tyrosine phosphorylation of DAP12 and the subsequent recruitment of Syk to the SIRPβ-DAP12 complex in RBL-2H3 cell transfectants (14). We have now shown that engagement of SIRPβ induced the tyrosine phosphorylation of DAP12 and its association with Syk in PEMs. It also elicited the phosphorylation of Syk, and a Syk inhibitor or kinase-negative Syk blocked the promotion of phagocytosis. A Syk inhibitor also blocked the activation of MAPK induced by SIRPβ engagement. The tyrosine phosphorylation of DAP12 and subsequent activation of Syk thus appear to contribute to the promotion of phagocytosis by ligation of SIRPβ. We also showed that engagement of SIRPβ induced the tyrosine phosphorylation of SLP-76 but not that of BLNK. In addition, this effect of SIRPβ on SLP-76 phosphorylation was blocked by a Syk inhibitor. SLP-76 was originally identified as a tyrosine-phosphorylated protein that bound to Grb2 in T cells (57). Subsequently, ZAP-70 and Syk were each shown to induce the tyrosine phosphorylation of SLP-76 (52, 53). SLP-76 forms a multiprotein complex with Grb2, Gads, LAT, phospholipase C-γ, Vas, and SLAP-130 (58). The association of SLP-76 with phospholipase C-γ and consequent activation of the latter would result sequentially in the generation of diacylglycerol, the activation of protein kinase C, and the activation of MEK. Indeed, the T cell receptor-mediated activation of MAPK was shown to be markedly attenuated in SLP-76-deficient T cells (59). It is thus possible that the engagement of SIRPβ activates the MEK-MAPK pathway, at least in part, through tyrosine phosphorylation of SLP-76.

We thus propose the following model for the signaling pathway activated by SIRPβ in the promotion of phagocytosis in macrophages (Fig. 9). Engagement of SIRPβ by its putative

ligand induces the tyrosine phosphorylation of DAP12 and the subsequent recruitment of Syk to DAP12 and its tyrosine phosphorylation. Activated Syk then mediates the tyrosine phosphorylation of SLP-76, which forms a multiprotein complex that triggers activation of the MEK-MAPK-MLCK cascade. MLC phosphorylation by MLCK increases myosin ATPase activity and elicits the reorganization of the actin cytoskeleton that underlies promotion of the phagocytic response.

The physiological ligand of SIRPβ remains to be identified. Although the extracellular regions of SHPS-1 and SIRPβ share sequence homology, recombinant SIRPβ-Fc does not bind the SHPS-1 ligand CD47[2] (12). The ligand for SIRPβ might be a soluble protein, such as IgG or complement, that binds to a phagocytic target. Alternatively, it might be a microbial component such as bacterial lipopolysaccharide or peptidoglycan, both of which are recognized by Toll-like receptors on macrophages or dendritic cells (3). Furthermore, a transmembrane protein on neighboring cells might interact with SIRPβ on macrophages to stimulate phagocytosis, as is the case with the adhesion molecule ICAM-1 on alveolar epithelial cells, which facilitates phagocytic activity of alveolar macrophages (60). Identification of its ligand should provide further insight into the physiological functions of SIRPβ.

Acknowledgments—We thank S. Shirahata, H. Yakura, J. Miyazaki, N. Honma, Y. Kaneko, K. Kohama, and H. Yamamura for reagents; H. Kobayashi, K. Tomizawa, and Y. Hayashi for technical assistance; and T. Takai, K. Sada, and E. Nishida for helpful discussions.

REFERENCES

1. Savill, J., and Fadok, V. (2000) *Nature* **407,** 784–788
2. Greenberg, S., and Grinstein, S. (2002) *Curr. Opin. Immunol.* **14,** 136–145
3. Medzhitov, R., and Janeway, C. A., Jr. (2002) *Science* **296,** 298–300
4. Platt, N., da Silva, R. P., and Gordon, S. (1998) *Trends Cell Biol.* **8,** 365–372
5. Cox, D., and Greenberg, S. (2001) *Semin. Immunol.* **13,** 339–345
6. Ravetch, J. V., and Bolland, S. (2001) *Annu. Rev. Immunol.* **19,** 275–290
7. Strzelecka, A., Kwiatkowska, K., and Sobota, A. (1997) *FEBS Lett.* **400,** 11–14
8. Caron, E., and Hall, A. (1998) *Science* **282,** 1717–1721
9. Aderem, A., and Underhill, D. M. (1999) *Annu. Rev. Immunol.* **17,** 593–623
10. Stephens, L., Ellson, C., and Hawkins, P. (2002) *Curr. Opin. Cell Biol.* **14,** 203–213
11. Kharitonenkov, A., Chen, Z., Sures, I., Wang, H., Schilling, J., and Ullrich, A. (1997) *Nature* **386,** 181–186
12. Seiffert, M., Brossart, P., Cant, C., Cella, M., Colonna, M., Brugger, W., Kanz, L., Ullrich, A., and Bühring, H. J. (2001) *Blood* **97,** 2741–2749
13. Dietrich, J., Cella, M., Seiffert, M., Bühring, H. J., and Colonna, M. (2000) *J. Immunol.* **164,** 9–12
14. Tomasello, E., Cant, C., Bühring, H. J., Vely, F., Andre, P., Seiffert, M., Ullrich, A., and Vivier, E. (2000) *Eur. J. Immunol.* **30,** 2147–2156
15. Lanier, L. L., Corliss, B., Wu, J., and Phillips, J. H. (1998) *Immunity* **8,** 693–701
16. Wu, J., Cherwinski, H., Spies, T., Phillips, J. H., and Lanier, L. L. (2000) *J. Exp. Med.* **192,** 1059–1068
17. Cant, C. A., and Ullrich, A. (2001) *Cell. Mol. Life Sci.* **58,** 117–124
18. Fujioka, Y., Matozaki, T., Noguchi, T., Iwamatsu, A., Yamao, T., Takahashi, N., Tsuda, M., Takada, T., and Kasuga, M. (1996) *Mol. Cell. Biol.* **16,** 6887–6899
19. Ohnishi, H., Kubota, M., Ohtake, A., Sato, K., and Sano, S. (1996) *J. Biol. Chem.* **271,** 25569–25574
20. Comu, S., Weng, W., Olinsky, S., Ishwad, P., Mi, Z., Hempel, J., Watkins, S., Lagenaur, C. F., and Narayanan, V. (1997) *J. Neurosci.* **17,** 8702–8710
21. Noguchi, T., Matozaki, T., Fujioka, Y., Yamao, T., Tsuda, M., Takada, T., and Kasuga, M. (1996) *J. Biol. Chem.* **271,** 27652–27658
22. Oshima, K., Ruhul Amin, A. R., Suzuki, A., Hamaguchi, M., and Matsuda, S. (2002) *FEBS Lett.* **519,** 1–7
23. Veillette, A., Thibaudeau, E., and Latour, S. (1998) *J. Biol. Chem.* **273,** 22719–22728
24. Seiffert, M., Cant, C., Chen, Z., Rappold, I., Brugger, W., Kanz, L., Brown, E. J., Ullrich, A., and Bühring, H. J. (1999) *Blood* **94,** 3633–3643
25. Brown, E. J., and Frazier, W. A. (2001) *Trends Cell Biol.* **11,** 130–135
26. Jiang, P., Lagenaur, C. F., and Narayanan, V. (1999) *J. Biol. Chem.* **274,** 559–562
27. Oldenborg, P. A., Zheleznyak, A., Fang, Y. F., Lagenaur, C. F., Gresham, H. D., and Lindberg, F. P. (2000) *Science* **288,** 2051–2054
28. Oldenborg, P. A., Gresham, H. D., and Lindberg, F. P. (2001) *J. Exp. Med.* **193,** 855–862
29. Aoki, N., Kimura, S., Takiyama, Y., Atsuta, Y., Abe, A., Sato, K., and Katagiri, M. (2000) *J. Immunol.* **165,** 3790–3796
30. Sato, R., Ohnishi, H., Kobayashi, H., Kiuchi, D., Hayashi, A., Kaneko, Y., Honma, N., Okazawa, H., Hirata, Y., and Matozaki, T. (2003) *Biochem. Biophys. Res. Commun.* **309,** 584–590
31. Yamao, T., Noguchi, T., Takeuchi, O., Nishiyama, U., Morita, H., Hagiwara, T., Akahori, H., Kato, T., Inagaki, K., Okazawa, H., Hayashi, Y., Matozaki, T., Takeda, K., Akira, S., and Kasuga, M. (2002) *J. Biol. Chem.* **277,** 39833–39839
32. Motegi, S., Okazawa, H., Ohnishi, H., Sato, R., Kaneko, Y., Kobayashi, H., Tomizawa, K., Ito, T., Honma, N., Bühring, H. J., Ishikawa, O., and Matozaki, T. (2003) *EMBO J.* **22,** 2634–2644
33. Williams, A. F., and Barclay, A. N. (1998) *Annu. Rev. Immunol.* **6,** 381–405
34. Ninomiya, N., Hazeki, K., Fukui, Y., Seya, T., Okada, T., Hazeki, O., and Ui, M. (1994) *J. Biol. Chem.* **269,** 22732–22737
35. Araki, N., Johnson, M. T., and Swanson, J. A. (1996) *J. Cell Biol.* **135,** 1249–1260
36. Karimi, K., and Lennartz, M. R. (1998) *Inflammation* **22,** 67–82
37. Mansfield, P. J., Shayman, J. A., and Boxer, L. A. (2000) *Blood* **95,** 2407–2412
38. Cantley, L. C. (2002) *Science* **296,** 1655–1657
39. Bhatt, N. Y., Kelley, T. W., Khramtsov, V. V., Wang, Y., Lam, G. K., Clanton, T. L., and Marsh, C. B. (2002) *J. Immunol.* **169,** 6427–6434
40. Dudley, D. T., Pang, L., Decker, S. J., Bridges, A. J., and Saltiel, A. R. (1995) *Proc. Natl. Acad. Sci. U. S. A.* **92,** 7686–7689
41. Favata, M. F., Horiuchi, K. Y., Manos, E. J., Daulerio, A. J., Stradley, D. A., Feeser, W. S., Van Dyk, D. E., Pitts, W. J., Earl, R. A., Hobbs, F., Copeland, R. A., Magolda, R. L., Scherle, P. A., and Trzaskos, J. M. (1998) *J. Biol. Chem.* **273,** 18623–18632
42. Yano, H., Nakanishi, S., Kimura, K., Hanai, N., Saitoh, Y., Fukui, Y., Nonomura, Y., and Matsuda, Y. (1993) *J. Biol. Chem.* **268,** 25846–25856
43. Klemke, R. L., Cai, S., Giannini, A. L., Gallagher, P. J., de Lanerolle, P., and Cheresh, D. A. (1997) *J. Cell Biol.* **137,** 481–492
44. Fincham, V. J., James, M., Frame, M. C., and Winder, S. J. (2000) *EMBO J.* **19,** 2911–2923
45. Saitoh, M., Ishikawa, T., Matsushima, S., Naka, M., and Hidaka, H. (1987) *J. Biol. Chem.*, **262,** 7796–7801
46. Olazabal, I. M., Caron, E., May, R. C., Schilling, K., Knecht, D. A., and Machesky, L. M. (2002) *Curr. Biol.* **12,** 1413–1418
47. Somlyo, A. V. (2002) *Circ. Res.* **91,** 83–84
48. Mitchison, T. J., and Cramer, L. P. (1996) *Cell* **84,** 371–379
49. Allen, L. A., and Aderem, A. (1996) *J. Exp. Med.* **184,** 627–637
50. Oliver, J. M., Burg, D. L., Wilson, B. S., McLaughlin, J. L., and McLaughlin, R. L. (1994) *J. Biol. Chem.* **269,** 29697–29703
51. Sada, K., Minami, Y., and Yamamura, H. (1997) *Eur. J. Biochem.* **248,** 827–833
52. Bubeck-Wardenburg, J., Pappu, R., Bu, J. Y., Mayer, B., Chernoff, J., Straus, D., and Chan, A. C. (1998) *Immunity* **9,** 607–616
53. Gross, B. S., Lee, J. R., Clements, J. L., Turner, M., Tybulewicz, V. L., Findell, P. R., Koretzky, G. A., and Watson, S. P. (1999) *J. Biol. Chem.* **274,** 5963–5971
54. Yablonski, D., and Weiss, A. (2001) *Adv. Immunol.* **79,** 93–128
55. Bonilla, F. A., Fujita, R. M., Pivniouk, V. I., Chan, A. C., and Geha, R. S. (2000) *Proc. Natl. Acad. Sci. U. S. A.* **97,** 1725–1730
56. Sano, S., Ohnishi, H., and Kubota, M. (1999) *Biochem. J.* **344,** 667–675
57. Jackman, J. K., Motto, D. G., Sun, Q., Tanemoto, M., Turck, C. W., Peltz, G. A., Koretzky, G. A., and Findell, P. R. (1995) *J. Biol. Chem.* **270,** 7029–7032
58. Liu, S. K.-W., Berry, D. M., and McGlade, C. J. (2001) *Oncogene* **20,** 6284–6290
59. Yablonski, D., Kuhne, M. R., Kadlecek, T., and Weiss, A. (1998) *Science* **281,** 413–416
60. Paine, R., III, Morris, S. B., Jin, H., Baleeiro, C. E., and Wilcoxen, S. E. (2002) *Am. J. Physiol.* **283,** L180–L187

[2] A. Hayashi, H. Ohnishi, and T. Matozaki, unpublished observations.

Positive Regulation of Phagocytosis by SIRPβ and Its Signaling Mechanism in Macrophages

Akiko Hayashi, Hiroshi Ohnishi, Hideki Okazawa, Seshiru Nakazawa, Hiroshi Ikeda, Sei-ichiro Motegi, Naoko Aoki, Shoji Kimura, Masahiko Mikuni and Takashi Matozaki

J. Biol. Chem. 2004, 279:29450-29460.
doi: 10.1074/jbc.M400950200 originally published online May 3, 2004
